International Journal of Performability Engineering, Vol. 10, No. 6, September 2014, pp. 577-588.

Printed in India

# Estimating Failure Intensity of a Repairable System to decide on its Preventive Maintenance or Retirement

RENYAN JIANG* and YANG GUO

*Faculty of Automotive and Mechanical Engineering Changsha University of Science and Technology, Changsha, Hunan 410114, China*

**Abstract:** Industrial equipment is usually repairable. Reliability of repairable systems depends on maintenance actions, and is characterized by mean cumulative function or failure intensity function of failure processes. Evolution trend of the failure intensity function is called the system-level failure pattern in the literature. The failure pattern plays an important role in preventive maintenance decision analysis. The purpose of this paper is to develop a robust non-parametric method to estimate the failure intensity function based on the failure processes observed from a single system or several independent and identical systems. After examining a large number of real-world datasets published in the literature, it is found that the intensity function of repairable systems is typically of roller-coaster curve shape. This type of failure pattern is illustrated and the possible causes are discussed. The usefulness for planning the preventive maintenance and determining the retirement time of repairable products is also illustrated.

***Keywords:*** *Repairable system, mean cumulative function, intensity function, failure pattern, non-parametric method*

## 1. Introduction

Products deteriorate with use. The deterioration results in a series of consequences. For example, operating and maintenance costs increase, energy consumption and pollution increase, and useful life decreases. Maintenance actions aim to moderate such consequences, and hence have a significant influence on product reliability and further on sustainability (*e.g.*, see [1]).

To effectively plan maintenance actions, one needs to understand the failure pattern of product, which refers to the evolution trend of the failure intensity function. As such, the failure pattern analysis is actually a kind of failure trend analysis. Jiang and Murthy [2] differentiate two kinds of failure patterns. One is associated with the failure rate function of non-repairable products, which is called the component-level failure pattern; and the other is associated with the failure intensity function (or rate of occurrence of failure) of repairable products, which is called the system-level failure pattern.

The trend analysis can play an important role in sustainability. In the use stage of a product, a preventive maintenance program is usually implemented and the product is subjected to a failure-repair process. During this process, the user accumulates a large amount of operation and reliability information. This kind of information can be used to carry out various analyses such as failure trend analysis, energy consumption trend analysis, operating and maintenance cost trend analysis, and trend analysis of various product sustainability indices (*e.g.*, see [3] and [4]). Such analyses can be integrated into eco-design tools to achieve sustainable product development [1], provide assistance in life-cycle assessment (a common approach to quantify environmental sustainability), and help to improve the future upgrades for existing products. In addition, the failure trend analysis and ownership cost analysis are particularly useful for optimizing preventive maintenance actions and making optimal product retirement decision. This can increase product life and operating efficiency and hence contributes to the product sustainability. In

*Corresponding author's email: jiang@csust.edu.cn

this paper, we focus on the reliability trend analysis of repairable systems, and the method to be presented can be applicable for the trend analysis for other performances or indices.

The literature on reliability of repairable systems is vast (*e.g.*, see [5] – [11]). Most of the literature uses the mean cumulative function (MCF) to characterize failure processes. MCF is the expected number of failures of a system or component in a given time interval, and the failure intensity function is the derivative of MCF. It is a common practice to directly model MCF and to indirectly derive the failure intensity function from MCF. To model MCF, one first examines the plot of empirical MCF using a non-parametric method so as to better understand the failure trend and help model selection. The empirical MCF obtained from real-world data often display complex shapes so that it is hard to find an appropriate parametric model for fitting the data. As such, the non-parametric method plays an important role in analyzing the reliability of repairable systems.

When the empirical MCF is obtained, it seems simple that the empirical intensity function can be obtained through applying a finite difference method to MCF. However, the empirical intensity function obtained in this way often sharply fluctuates, as shown in Figure 1 (where $m(t)$ is the intensity function and defined in Eq. (2)), so that it is hard to identify the evolution trend. As such, it is desired to develop a robust non-parametric method for estimating intensity function. This paper addresses this issue.

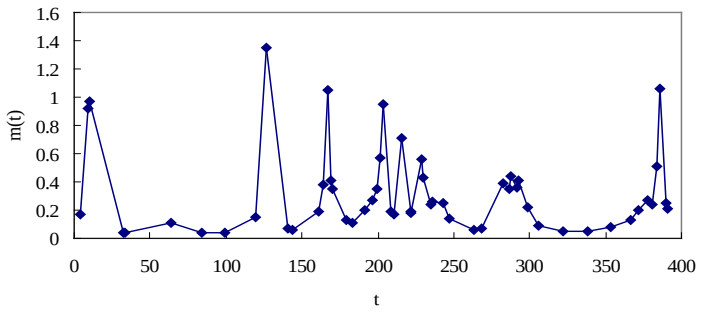


**Figure 1:** An Empirical Intensity Function derived from an Empirical MCF

The fluctuation problem results from small inter-failure times. The basic idea to solve this problem is to replace individual data points in the empirical MCF with the average point of the data points close to each other by grouping the data to intervals. Two closely-linked issues are (a) grouping data to interval and (b) averaging grouped data.

Law and Kelton [12] present a nonparametric method to estimate the intensity function. The method divides the time axis into non-overlapping time intervals, assumes that the intensity function is a constant in each interval, and the interval average intensity is estimated based on the number of failures occurred in this time interval. The key of this method is how to partition intervals so as to have enough data points in each interval. In addition, it is only applicable for the cases where the systems have a common observation window, implying that the number of the systems does not change with time.

Leemis [13] proposes a piecewise-linear MCF model, which can be used to generate a point process for Monte Carlo simulation. Similarly, the method is only applicable for the cases where the number of the systems does not change with time.

Arkin and Leemis [14] extend the piecewise-linear MCF model to the piecewise-linear intensity model (*i.e.*, quadratic MCF). The intervals are partitioned so that the number of systems in each interval keeps unchanged. This leads to the case where there may be no failure in some time intervals or the interval length may be too small.

In this paper, we present a nonparametric method to estimate the intensity function. In principle, the proposed method is similar to the method of Law and Kelton [12] but there are differences in the following two aspects. Firstly, the proposed method is applicable for the case where the number of systems changes with time. Secondly, the proposed method provides specific details to determine the boundaries between successive intervals. Based on pre-specified rules, we first divide the observed time window into several equal-space intervals and then those intervals with many data points are further subdivided into a few equal-space sub-intervals. For a given interval or sub-interval, we estimate the MCF of a representative point or average point. Using the central difference method, the empirical intensity function is derived from the estimated MCF. This is an indirect method to estimate the interval average intensity.

Applying the proposed method to a large number of real-world datasets, we find that the empirical failure intensity function is typically of roller-coaster curve shape. Some simpler shapes such as unimodal, bimodal, unimodal-followed-by-increasing and decreasing-followed-by-unimodal shapes can be viewed as its truncated cases. In other words, they will become the roller-coaster curve if the observation continues. Four real-world examples are analyzed in detail and other four examples are given in Appendix to illustrate the proposed method and findings. We also discuss the causes that lead to the roller-coaster curve.

The paper is organized as follows. The proposed approach is presented in Section 2 and illustrated in Section 3. The causes that lead to the roller-coaster curve are explained in Section 4. The paper is concluded in Section 5.

## 2. Proposed Approach

### 2.1 MCF and Failure Intensity Function

Consider $n$ nominally identical repairable systems. Let $N_i(t)$ denote the number of failures of the $i$-th system in $[0,t]$, which is a random variable. MCF is the expected failure number in $(0,t)$ *per system, i.e.,* $M(t) = E[N(t)]$, where

$$N(t) = \frac{1}{n}\sum_{i=1}^{n} N_i(t). \tag{1}$$

The failure intensity function is defined as

$$m(t) = dM(t)/dt. \tag{2}$$

According to Eq. (2), $m(t)\Delta t$ describes the expected number of failures per system within the interval $(t, t+\Delta t)$.

The above definitions do not depend on whether the system is subjected to a preventive maintenance (PM) program or not. If the system is subjected to a PM program, MCF obtained from the field data actually reflects its effect. As a result, two main factors that affect MCF or intensity function are the underlying life distribution (*i.e.*, inherent reliability) and the maintenance actions (including their frequency, depth and efficiency). There are other influence factors, which will be discussed in Section 4.

### 2.2 Non-parametric Estimation for MCF

Assume that the failure point process of the $i$-th system is given by

$$(t_{ij}; 1 \le j \le n_i, 1 \le i \le n). \tag{3}$$

For all the $n$ failure point processes, we arrange all the failure times in an ascending order as follows:

$$(t_k, k = 1, 2, ..., m = \sum_{i=1}^{n} n_i) \tag{4}$$

Let $s_k$ denote the number of the systems that are under observation at $t_k$. In time interval $(t_{k-1}, t_k)$ (which does not include $t_k$), there is no failure and hence we have

$$M(t_k^-) = M(t_{k-1}^+), \quad M(t_0 = 0) = 0. \tag{5}$$

In time interval $(t_{k-1}, t_k]$, there is a failure at $t_k$ among $s_k$ systems, and hence MCF increases by $1/s_k$. As a result, we have the following recursive relation:

$$M(t_k^+) = M(t_{k-1}^+) + \frac{1}{s_k}. \tag{6}$$

Since MCF has a jump at each failure instant $t_k$, we use their average as the representative value of MCF at $t_k$, *i.e.*,

$$M(t_k) = [M(t_k^-) + M(t_k^+)]/2. \tag{7}$$

Eq. (7) can be graphically displayed by drawing $M(t_k)$ versus $t_k$.

Specially, for a single system, we have $s_k = 1$ and $M(t_k) = k$. In this case, the TTT plot of a repairable system (*e.g.*, see [15]) is actually the plot of $t_k$ versus $M(t_k)$. In this sense, MCF plot can be viewed as a generalized TTT plot, which is not normalized to 1.

### 2.3 Example 1

The data shown in Table 1 deal with the failure process of the power-train system of a bus ([16]), and the observation is truncated at $t = 394.064 \times 10^3$ km. Using the approach outlined above, we obtained the plot of MCF shown in Figure 2. As seen, the system deteriorates in a complex way.

**Table 1: Failure Times (1000 km) of the Power-train System of Bus 510 ([16])**

| | | | | | | | |
|---|---|---|---|---|---|---|---|
| 7.780 | 9.061 | 9.962 | 11.120 | 54.849 | 56.087 | 72.806 | 112.779 |
| 125.519 | 126.474 | 127.005 | 155.387 | 161.325 | 165.737 | 166.535 | 167.647 |
| 171.418 | 173.284 | 186.644 | 192.288 | 196.434 | 199.785 | 202.197 | 203.264 |
| 204.298 | 213.968 | 216.055 | 216.786 | 226.757 | 227.718 | 230.351 | 232.384 |
| 238.659 | 240.092 | 246.691 | 254.052 | 280.350 | 283.321 | 285.472 | 288.990 |
| 289.974 | 294.528 | 294.816 | 303.694 | 317.602 | 340.085 | 358.340 | 366.740 |
| 374.316 | 376.794 | 381.824 | 385.066 | 385.730 | 386.947 | 393.885 | **394.064+** |

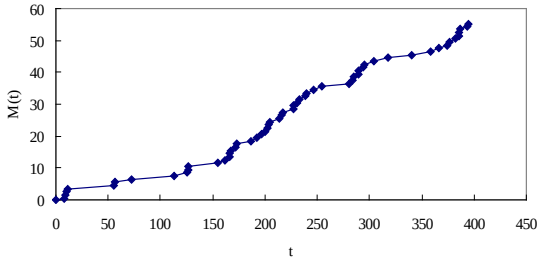


**Figure 2:** MCF of Example 1

To examine the failure intensity, a simple method is to replace the derivative of Eq. (2) by the central difference given by

$$m(\bar{t}_k) \approx \frac{M(t_{k+1}) - M(t_{k-1})}{t_{k+1} - t_{k-1}}, \quad \bar{t}_k = \frac{t_{k-1} + t_{k+1}}{2}. \tag{8}$$

From Eq. (8) we obtained the plot of the empirical intensity function, which has been shown in Figure 1. As mentioned earlier, the plot fluctuates so that it is hard to determine the failure evolution trend. To improve, we propose two approaches as follows.

### 2.4 Interval Average Intensity

Consider the dataset given by Eq. (4) in the observation window $(0, t_s]$, where $t_s$ $(\geq t_m)$ can be a failure or censored time. We divide the interval $(0, t_s)$ into $g$ equal-space intervals with the interval length $\Delta = t_s / g$. The interval number $g$ is determined so that each interval at least contains a data point. Letting $\Delta_0 = \max(t_j - t_{j-1}; 1 \leq j \leq n)$, we have $g = \text{int}(t_s / \Delta_0)$. As such, the interval boundaries are given by

$$\tau_j = j\Delta, 0 \leq j \leq g. \tag{9}$$

MCF at each boundary point can be estimated using linear interpolation ([12]). The interval average intensity in the $j$-th interval is given by

$$m(t) = \frac{M(\tau_j) - M(\tau_{j-1})}{\Delta}, \quad t \in ((j-1)\Delta, j\Delta). \tag{10}$$

To illustrate, we look at the data in Example 1. For this example, we have $\Delta_0 = 43.73$ and $g = 9$. The interval average intensity function is shown in Figure 3. As seen, the fluctuation gets significant improvement but the smoothness can be further improved.

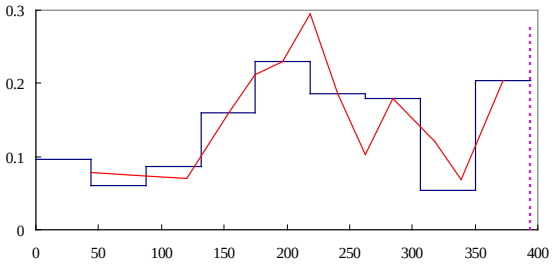


**Figure 3:** Interval Average Intensity Function for Example 1

### 2.5 Difference Method for Adjusted MCF

We improve the smoothness by merging the points of MCF that are close to each other using averaging.

In Section 2.4, we have divided the data points to $g$ intervals. In some intervals, the number of the data points can be small (*e.g.*, smaller than or equal to 5). In this case, we directly average the values of $t$ and $M(t)$ of the data points in an interval, respectively, and use the average point to replace those data points. If the number of the data points is larger than 5, we further divide the interval into $k_j$ subintervals and the value of $k_j$ is empirically determined by the following

$$k_j = 1 + \text{int}(\frac{n_j}{6}) \tag{11}$$

where $\text{int}(x)$ is the largest integer part of $x$. For each subinterval, we use the average point to replace those data points in the subinterval. As such, we obtain the adjusted MCF. The empirical failure intensity is obtained using Eq. (8) for the adjusted MCF.

To illustrate, we look at the data in Example 1 again. Using the approach outlined above, we obtained the adjusted MCF shown in Figure 4. Compared with Figure 2, the distribution of the data points is much more uniformed. Applying the adjusted MCF to Eq. (8), we obtained the empirical intensity function shown in Figure 3. As seen, there is a good agreement between the intensity functions obtained from the two approaches; and it is clear that the failure intensity function looks like a roller-coaster curve [17].

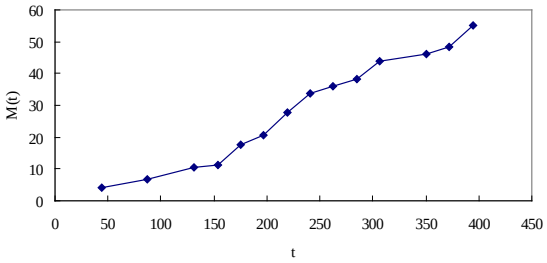


**Figure 4:** Adjusted MCF for Example 1

## 3. Roller-Coaster Curve as a Typical Failure Pattern

To further confirm the roller-coaster failure intensity pattern, we look at three more examples as follows.

### 3.1 Example 2

The data shown in Table 2 deal with the failure process of the power-train system of another bus ([18]). Similar analysis has been carried out for this dataset, and found that the failure pattern is similar to the one shown in Figure 3. As such, we analyze the data pooled from Tables 1 and 2 so as to obtain more refined results. For the pooled data, the empirical intensity functions obtained from the two approaches are shown in Figure 5. As seen, the intensity function curve somehow looks like the superposition of two bathtub curves, and the flat part in the second bathtub curve is greater than the flat part of the first. This implies that the bus has to be retired after a few overhauls.

It appears reasonable to schedule the first overhaul at about 160,000 km. If this was really implemented, the intensity function after this time point would be different from the one shown in Figure 5. In other words, the intensity function is not the inherent property of a repairable system since it strongly depends on the history of maintenance.

**Table 2: Failure Times (1000 km) of the Power-train System of Bus 514 ([18])**

| | | | | | | | |
|---|---|---|---|---|---|---|---|
| 2.412 | 3.206 | 4.390 | 12.584 | 29.909 | 50.712 | 98.550 | 101.072 |
| 144.493 | 159.216 | 162.417 | 178.513 | 205.731 | 206.638 | 217.134 | 217.676 |
| 219.244 | 219.587 | 221.768 | 224.582 | 231.228 | 233.284 | 240.828 | 245.922 |
| 261.928 | 262.744 | 295.685 | 297.978 | 304.640 | 306.578 | 310.752 | 331.517 |
| 333.796 | 337.552 | 347.035 | **365.477**+ | | | | |

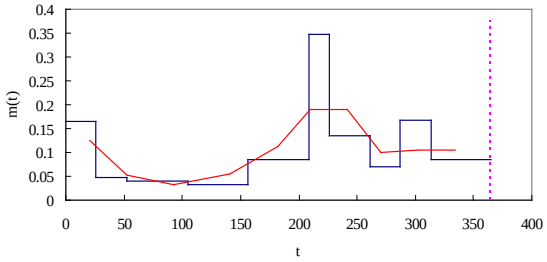


**Figure 5:** Empirical Intensity Function for Example 2

### 3.2 Example 3

The data shown in Table 3 deal with failure times of the hydra systems of five LHD machines ([19] and [20]).

**Table 3: Failure Times (in hours) of Hydra Systems of LHD Machines ([19] and [20])**

| LHD1 | LHD3 | | LHD09 | | LHD11 | | LHD17 | |
|---|---|---|---|---|---|---|---|---|
| 327 | 637 | 3386 | 278 | 4361 | 353 | 2197 | 401 | 2890 |
| 452 | 677 | 3526 | 539 | 4371 | 449 | 2456 | 437 | 3108 |
| 459 | 1074 | | 1529 | 4682 | 498 | 2739 | 455 | 3230 |
| 465 | 1110 | | 1720 | 4743 | 709 | 2889 | 614 | |
| 572 | 1164 | | 1827 | | 791 | 2913 | 955 | |
| 849 | 1217 | | 1859 | | 966 | | 1126 | |
| 903 | 1314 | | 1910 | | 1045 | | 1150 | |
| 1235 | 1377 | | 1920 | | 1162 | | 1500 | |
| 1745 | 1593 | | 2052 | | 1188 | | 1572 | |
| 1855 | 1711 | | 2228 | | 1192 | | 1875 | |
| 1865 | 1836 | | 2475 | | 1197 | | 1909 | |
| 1874 | 1861 | | 2640 | | 1257 | | 1954 | |
| 1959 | 1865 | | 3094 | | 1296 | | 2278 | |
| 1986 | 1966 | | 3236 | | 1331 | | 2280 | |
| 2045 | 2150 | | 3274 | | 1589 | | 2350 | |
| 2061 | 2317 | | 3523 | | 1686 | | 2407 | |
| 2069 | 2398 | | 3735 | | 1745 | | 2510 | |
| 2103 | 2444 | | 3939 | | 1748 | | 2521 | |
| 2124 | 2462 | | 4121 | | 1785 | | 2526 | |
| 2276 | 2494 | | 4237 | | 1793 | | 2529 | |
| 2434 | 2713 | | 4267 | | 2038 | | 2673 | |
| 2478 | 3118 | | 4291 | | 2117 | | 2753 | |
| 2496 | 3138 | | 4323 | | 2166 | | 2806 | |

The empirical intensity function is shown in Figure 6. As seen, it has five peaks. A careful examination finds that two overhauls can be scheduled at about 1700 and 4000 hours so as to reduce failures.

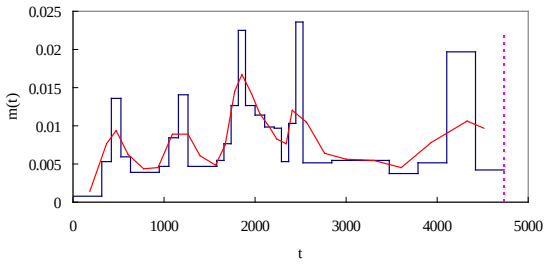


**Figure 6:** Empirical Intensity Function for Example 3

### 3.3 Example 4

The data shown in Table 4 come from [21] and deal with failure times of locomotive traction motors. The empirical intensity function of the failure process is shown in Figure 7, which can be roughly viewed as being decreasing-followed-by-unimodal. As seen from the figure, the reliability can be improved by conducting a burn-in test and by completing an overhaul at about 5000 hours.

**Table 4: Failure Times (in hours) of Locomotive Traction Motors ([21])**

| | | | | | | | |
|---|---|---|---|---|---|---|---|
| 166 | 201 | 450 | 640 | 667 | 708 | 767 | 842 |
| 1065 | 2017 | 2352 | 2516 | 2661 | 2831 | 2971 | 3469 |
| 4040 | 4539 | 4879 | 5039 | 5167 | 5198 | 5263 | 5484 |
| 5800 | 5822 | 6083 | 6115 | 6512 | 6560 | 6561 | 6588 |
| 6883 | 7023 | 7850 | 7852 | 8061 | 8090 | 8256 | 9456 |

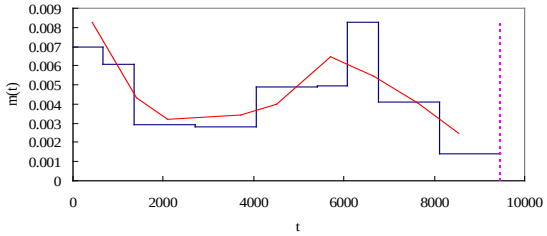


**Figure 7:** Empirical intensity function for Example 4

## 4. Engineering Significance of Roller-Coaster Failure Pattern

After having analyzed many datasets, we found that the intensity function alternately increases [decreases] and decreases [increases] in many cases, *i.e.*, roller-coaster pattern. The examples with this failure pattern include the failure of load-haul-dump (LHD) machines [18] and the failure of air-conditioning/cooling packs [22]. Their failure intensity curves are displayed in Figures A2 and A3 in Appendix.

This pattern usually appears when the observation window is large, and results from the following causes:

- ♦ It is well-known that manufacturing defects and aging can lead to a bathtub intensity curve.

- The maintenance action leads to a decrease in the intensity so that the continuous improvement in maintenance management can lead to a unimoal failure intensity curve.
- Failure replacements of key components generate renewal processes. The renewal intensity function oscillates when the dispersion of the life distribution is relatively small (*e.g.*, see [23]). This is because the failures more possibly occur at the times that are integer times of the component mean life. The oscillation phenomenon may occur for the repairs with the effects close to being perfect.
- Cyclic factors such as climate conditions can significantly impact the field reliability (*e.g.*, see [24]). In this case, the intensity function periodically oscillates.

The combination of the above factors leads to the intensity function oscillating in a complex way. Generally, the influence of manufacturing defects and the oscillation phenomenon due to components' replacements decrease with time, the aging phenomenon eventually becomes a major influence factor so that the product has to be overhauled or retired. As such, product failure intensity analysis can help to optimize the product overhaul and retirement decisions.

When the observation window is not large enough, we will see a part of the roller-coaster curve. In this case, the observed failure pattern can be unimodal, bimodal, bathtub-shaped, unimodal-followed-by-increasing or decreasing-followed-by-unimodal. For example, the failure process of a compressor system on an offshore installation [19] displays a bimodal failure pattern; the failure pattern of the locomotive traction motors in Example 4 is decreasing-followed-by-unimodal; and Figure A4 in Appendix displays a the unimodal-followed-by-increasing failure pattern.

## 5. Conclusions

In this paper, we have proposed a non-parametric method to estimate the failure intensity function of a single or multiple identical repairable products. The proposed method is applicable for the situations where the number of the systems under observation changes with time. The proposed method is robust in terms of the identifiability of evolution trend and the smoothness of the empirical intensity function, and can be easily implemented in Microsoft Excel. It is also applicable for both new and reconditioned (or remanufactured) products.

A main finding is that the failure intensity function is typically roller-coaster curve shaped if the observation time is long enough. A number of other patterns can be viewed as its truncated cases. The main causes for this pattern include manufacturing defects, replacements of components, maintenance improvement, the influence of external cyclic factors and product aging. Through the failure intensity analysis, appropriate time period for possible burn-in test and appropriate time instants for higher-level preventive maintenance actions can be obtained. The analysis is also useful for the assessment and analysis of product sustainability.

A topic for future research is to summarize typical failure patterns through analyzing a large number of real-world datasets. We are working on this topic.

## Appendix: Additional Examples of Roller-Coaster Failure Intensity Pattern

Four empirical failure intensity curves with the roller-coaster failure pattern are displayed in Figures A1 through A4, and the data for generating these plots come from References [14], [18], [22] and [25], respectively.

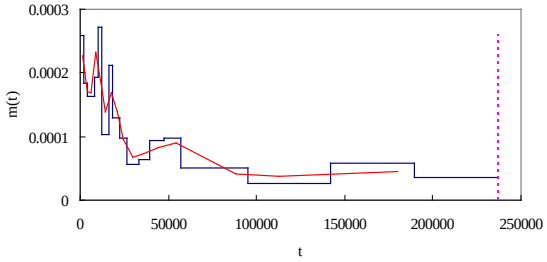


**Figure A1:** Failure Intensity of Photocopiers

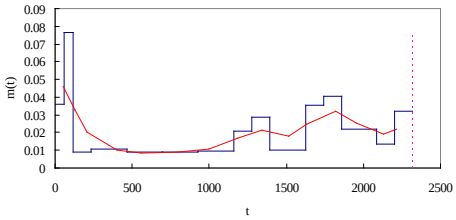


**Figure A2:** Failure Intensity of a Load-Haul-Dump Machine (LHD-A, [18])

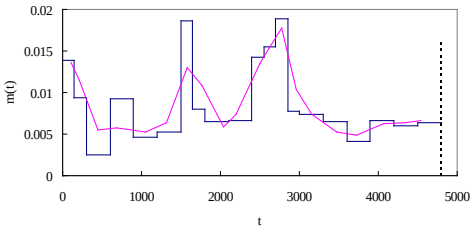


**Figure A3:** Failure Intensity of an Aircraft Air-conditioning/Cooling Packs

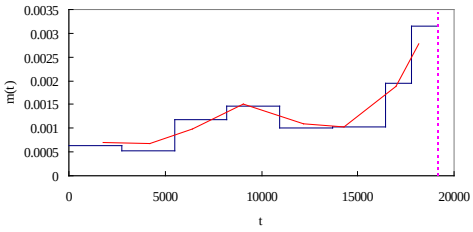


**Figure A4:** Failure Intensity of a Main Propulsion Motor

**Acknowledgement:** The authors would like to thank the Guest Editors, the Editor–in-Chief and referees for their helpful comments and suggestions which have greatly enhanced the clarity of the paper. The research was supported by the National Natural Science Foundation (No. 71071026 and No. 71371035).

## References


[1] Ramani, K., D. Ramanujan, W. Z. Bernstein, F. Zhao, J. Sutherland, C. Handwerker, J. K. Choi, H. Kim, and D. Thurston. *Integrated Sustainable Life Cycle Design: A Review*. Journal of Mechanical Design, 2010; 132: 1-15.

[2] Jiang, R., and D. N. P. Murthy. *Maintenance: Decision Models for Management*. Science Press, Beijing, 2008.

[3] Loucks, D. P. *Quantifying Trends in System Sustainability*. Hydrological Sciences Journal, 1997; 42(4): 513-530.

[4] Singh, R. K., H. R. Murty, S. K. Gupta, and A. K. Dikshit. *An Overview of Sustainability Assessment Methodologies*. Ecological Indicators, 2009; 9: 189-212.

[5] Cox, D., and P. Lewis. *The Statistical Analysis of Series of Events*. Chapman & Hall, London, 1966.

[6] Crow, L.H.. *Reliability Analysis of Complex Repairable Systems*. In *Reliability and Biometry*, ed. F. Proschan and R. J. Serfling, Philadelphia: SIAM, 1974; 379-410.

[7] Ascher, H., and H. Feingold. *Repairable Systems Reliability: Modeling, Inference, Misconceptions and Their Causes*. Marcel Dekker, New York, 1984.

[8] Rigdon, S. E., and A. P. Basu. *The Power Law Process: A Model for the Reliability of Repairable Systems.* Journal of Quality Technology, 1989; 21(6): 251-260.

[9] Jiang, R. *Three Extended Geometric Process Models for Modeling Reliability Deterioration and Improvement*. International Journal of Reliability and Applications, 2011; 12(1): 49-60.

[10] Jiang, R., and C. Huang. *Failure Patterns of Repairable Systems and a Flexible Intensity Function Model*. International Journal of Reliability and Applications, 2012; 13(2): 81-90.

[11] Jiang, R. *Life Restoration Degree of Minimal Repair and Its Applications*. Journal of Quality in Maintenance Engineering, 2013; 19(4): 413-428.

[12] Law, A. M., and W. D. Kelton. *Simulation Modeling and Analysis*. McGraw-Hill, New York, 2nd ed, 1991; 407.

[13] Leemis, L. M. *Nonparametric Estimation of the Cumulative Intensity Function for a Nonhomogeneous Poisson Process*. Management Science, 1991; 37(7): 886-900.

[14] Arkin, B. L., and L. M. Leemis. *Nonparametric Estimation of the Cumulative Intensity Function for a Nonhomogeneous Poisson Process from Overlapping Realizations.* Management Science, 2000; 46(7): 989-998.

[15] Kvaløy, J. T., and B. H. Lindqvist. *TTT-based Tests for Trend in Repairable System Data*. Reliability Engineering and System Safety, 1998; 60: 13-28.

[16] Guida, M., and G. Pulcini. *Reliability Analysis of Mechanical Systems with Bounded and Bathtub Shaped Intensity Function*. IEEE Transactions on Reliability, 2009; 58(3): 432-43.

[17] Wong, K. L., and D. L. Lindstrom. *Off the Bathtub onto the Roller-coaster Curve*. The 1988 Proceedings of Annual Reliability & Maintainability Symposium, Los Angeles, Jan 26-28, 1988; 356-363.

[18] Kumar, U., B. Klefsjo, and S. Granholm. *Reliability Investigation for a Fleet of Load Haul Dump Machines in a Swedish Mine*. Reliability Engineering and System Safety, 1989; 26: 341-361.

[19] Blischke, W. R., M. R. Karim, and D. N. P. Murthy. *Warranty Data Collection and Analysis*. Springer, New York, 2011.

[20] Attardi, L., and G. Pulcini. *A New Model for Repairable Systems with Bounded Failure Intensity*. IEEE Transactions on Reliability, 2005; 54(4): 572-582.

[21] Jung, M., and D. S. Bai. *Analysis of Field Data under Two-dimensional Warranty*. Reliability Engineering and System Safety, 2007; 92: 135-143.
[22] Al-Garni, A. Z., M. Tozan, A .M. Al-Garni, and A. Jamal. *Failure Forecasting of Aircraft Air-Conditioning/Cooling Pack with Field Data*. Journal of Aircraft, 2007; 44(3): 996-1002.
[23] Jiang, R. *A Gamma-normal Series Truncation Approximation for Computing the Weibull Renewal Function*. Reliability Engineering and System Safety, 2008; 93: 616-626.
[24] Jiang, R., Y. Liao, and C. Fei. *Impact of Climate Conditions on Field Reliability of Vehicles*. Applied Mechanics and Materials, 2012; 121-126: 3335-3339.
[25] Yañez, M., F. Joglar, and M. Modarres. *Generalized Renewal Process for Analysis of Repairable Systems with Limited Failure Experience*. Reliability Engineering and System Safety, 2002; 77: 167-180.

**Renyan Jiang** is Professor and Director of the Quality, Reliability and Maintenance Laboratory at Changsha University of Science and Technology, China. Prof. Jiang got his Ph.D. at University of Queensland, Australia. His research interests are in various aspects of quality, reliability and maintenance. He has authored or co-authored four reliability related books, and published more than 60 papers in international journals.